IEEE 2010© 978-1-4244-6890-4/10$26.00

Design and Analysis of High Efficiency DC-DC Boost Converter with Active Resonant Technique for Small Grid-Connected PV Systems

Damrong Amorndechaphon
Electrical Engineering Department
Phayao University
Phayao, Thailand
a_damrong@hotmail.com

Suttichai Premrudeepreechacharn
Electrical Engineering Department
Chiangmai University
Chiangmai, Thailand
suttic@gmail.com

Kohji Higuchi
Department of Electronic Engineering
The University of Electro-Communications
Chofu, Tokyo, Japan
higuchi@ee.uec.ac.jp

***Abstract*—In this paper, an analytical analysis and design of an active resonant snubber that is used for reducing the switching loss and switching stress of the dc-dc boost converter in grid-connected PV systems is proposed. The operation principle of the proposed active snubber is analyzed. A design consideration is developed according to the equations derived in various operation stages for determining the optimized values of soft commutation circuit components. The performance of the grid-connected PV system with the soft-switching dc-dc boost converter is demonstrated by simulation results to verify the operation analysis and the efficiency improvement. The results show that less switching loss and switching stress of the converter switch are obtained by the proposed active resonant scheme. The overall efficiency of an improved dc-dc boost converter is increased to about 94% from the value of 93% in its hard-switching PWM counterpart.**

Keywords-Soft-switching; grid-connected inverter; active resonant snubber.

I. INTRODUCTION

This recent years, the conventional PWM inverter shown in figure 1 has been widely used for small grid-connected PV-system (<10kW) due to the individual operation and simple control [1]. These systems are composed of PV arrays, a dc-dc converter and a dc-ac inverter. To minimize the size and weight of overall system, high switching frequency operation is required for inverter. Unfortunately, increased switching frequency causes higher switching losses and greater electromagnetic interference (EMI). To overcome these problems, the soft-switching techniques are widely applied, which can also improve the EMI of the systems. Soft-switching techniques can be divided into two main categories, active soft-switching and passive soft-switching, which have different technical characteristics. Both of soft-switching techniques have been presented by adding resonant snubbers to the conventional PWM converters. The passive resonant snubber seem to be attractive, for not requiring auxiliary switch and associated timing and driving circuits, some previous works [2] successfully achieve soft-switching at turn-on and turn-off without voltage stresses. However, their current stresses during turn-on are increased, and their designs are relatively complicated. In practical, the duty cycle range of the PWM converter with passive resonant snubber is limited by the soft-switching resonant commutation. To solve these problems, various active resonant techniques have been proposed in recent years [3-4]. It is generally implemented by adding an active resonant snubber, which employ resonant techniques. This snubber combines the desirable features of both the conventional PWM and soft switching resonant technique. Through this method, the switching stress is reduced because the switching devices are clamped the same way as its conventional PWM counterpart. The switching losses and EMI are also reduced because the converters operate at either ZVS or ZCS.

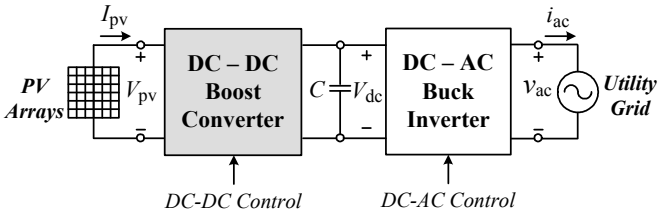

Figure 1. Power converter topology for conventional small grid-connected PV-systems.

In this paper, a design and analytical analysis of dc-dc boost converter with active resonant technique for small grid-connected PV systems is presented to reduce the switching loss and switching stress of the semiconductor switches. Its operation principle is analyzed, the design considerations are also discussed, and the simulation circuit has been designed to test and verify the performance of this proposed technique

II. PRINCIPLE OF OPERATION

A. Definitions and assumptions

The proposed dc-dc boost converter with active snubber is shown in figure 2. The active snubber circuit consists of an auxiliary switch S_a, resonant inductor L_r, resonant capacitor C_r, and diode D_1. To simplify the steady-state analysis of the circuit during one switching cycle, the following conditions and assumption are made:

This work was supported in part by Thailand Research Fund (TRF) through the Royal Golden Jubilee Ph.D. program under grant No. PHD/0166/2550.

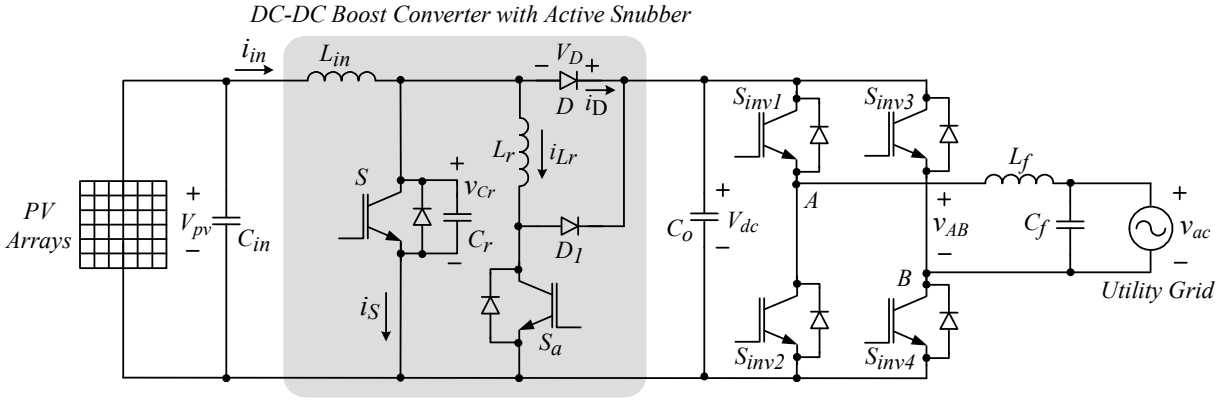

Figure 2. Developed dc-dc boost converter with active resonant technique for small grid-connected PV-systems.

1. The boost inductor is large enough, the inductor current can be considered as a constant current source, I_{in}.

2. The output capacitor is large enough to be treated as constant voltage source, V_{dc}.

3. Semiconductor switches are ideal.

3.1 No forward voltage drops in the on-state.

3.2 No leakage current in the off-state.

3.3 No time delay at both turn-on and turn-off.

4. Passive components of the resonant circuit are ideal.

B. Operation stages

In steady-state operation, a complete switching cycle can be divided into seven stages. The key waveforms and their equivalent circuits are shown in figure 3 and figure 4, respectively. A detailed analysis of every stage is presented below.

1) Stage 1 ($t < t_0$): In this stage, the main switch S and the auxiliary switch S_a are off, the main diode D is conducting. The input current I_{in} flows to V_{dc} through the main diode D. At this stage, the resonant inductor current $i_{Lr}(t)$ and the resonant capacitor $v_{Cr}(t)$ can be expressed as follows:

$$i_{Lr}(t) = 0 \tag{1}$$

$$v_{Cr}(t) = V_{dc} \tag{2}$$

2) Stage 2 ($t_0 - t_1$): At $t = t_0$, the auxiliary switch S_a is turned on, and the resonant inductor L_r current increases linearly, while the D current decreases gradually. S_a is turned on under zero-current-switching (ZCS). At $t = t_1$, the resonant inductor current $i_{Lr}(t)$ reaches I_{in} and the main diode current i_D drops to zero. So the main diode D is naturally turned off with ZCS. The reverse current of D is negligible if a fast switching diode is employed. Therefore, the circuit equations and initial conditions in this stage are given as follows:

$$L_r \frac{di_{Lr}(t)}{dt} = V_{dc} \tag{3}$$

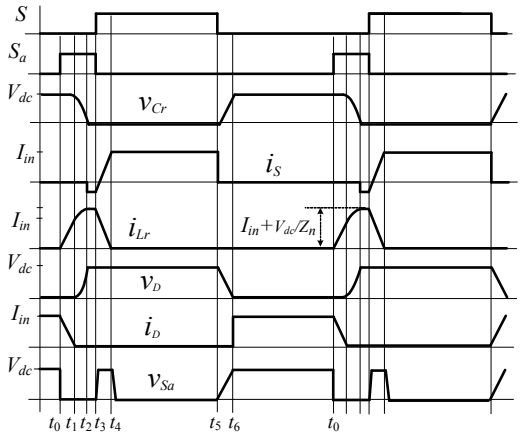

Figure 3. Theoretical waveforms of the proposed dc-dc boost converter.

$$C_r \frac{dv_{Cr}(t)}{dt} = 0 \tag{4}$$

$$i_{Lr}(t_0) = 0 \tag{5}$$

$$v_{Cr}(t_0) = V_{dc} \tag{6}$$

The solutions are determined as follows:

$$i_{Lr}(t) = \frac{V_{dc}}{L_r} t \tag{7}$$

$$v_{Cr}(t) = V_{dc} \tag{8}$$

The resonant inductor current i_{Lr}(t) reaches I_{in} at $t = t_1$. Thus, the time interval of this stage can be solved to be

$$\Delta t_{01} = t_1 - t_0 = (L_r . I_{in}) / V_{dc} \tag{9}$$

3) Stage 3 ($t_1 - t_2$): At $t = t_1$, a parallel resonant occurs via the resonant path L_r -C_r under constant input current I_{in}. The resonant inductor current $i_{Lr}(t)$ continues to increase and reaches its maximum value at $t = t_2$, while the voltage $v_{Cr}(t)$ across the resonant capacitor is decreased from V_{dc} to zero at $t = t_2$. This mode ends when $v_{Cr}(t)$ becomes zero. The equations and initial conditions that characterize this interval are described as follows:

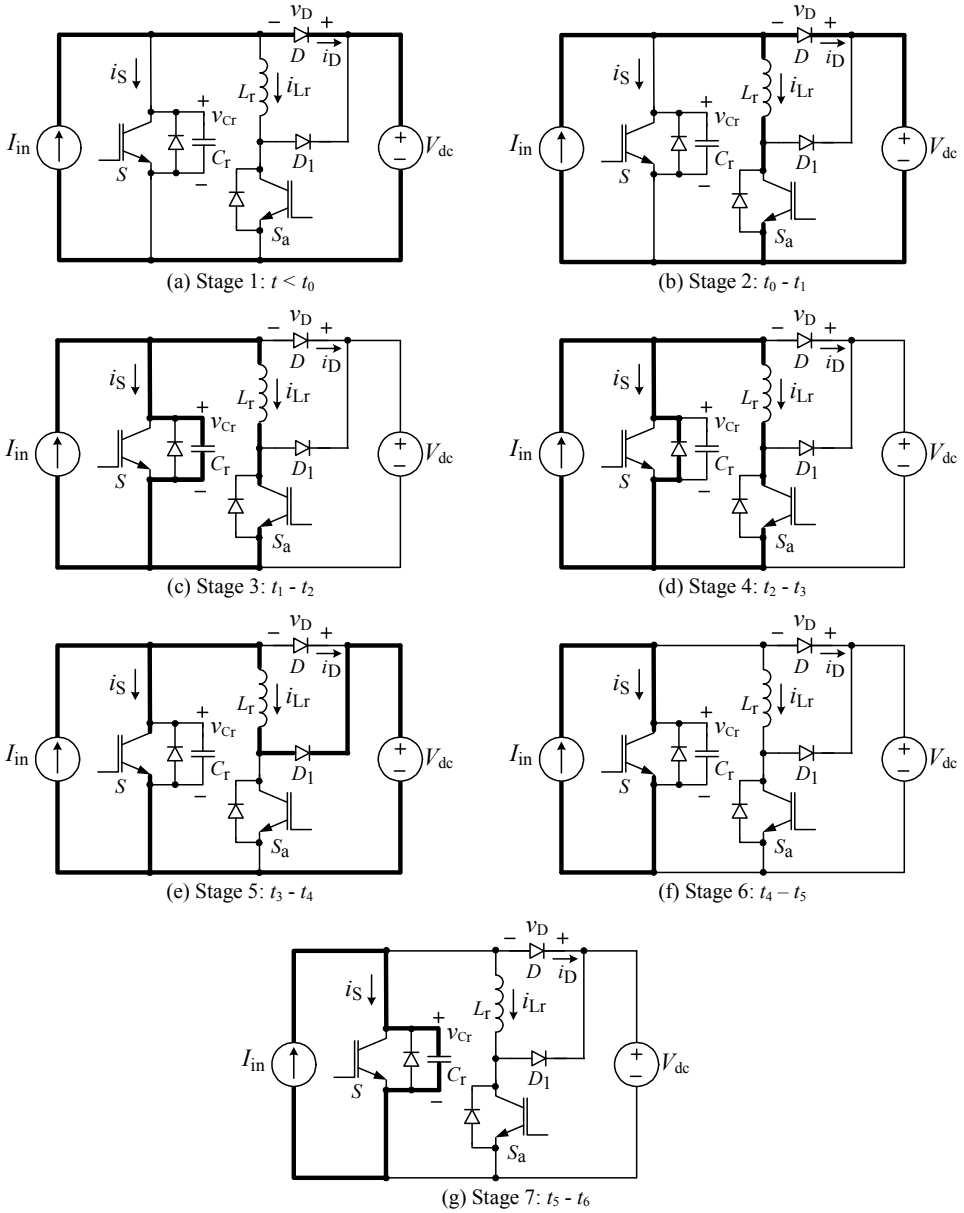

Figure 4. The operation stages in one switching cycle.

$$i_{Lr}(t) = I_{in} - i_{Cr}(t) = I_{in} - C_r \frac{dv_{Cr}(t)}{dt} \tag{10}$$

$$v_{Cr}(t) = \frac{1}{C_r}\int i_{Cr}(t)dt \tag{11}$$

$$i_{Lr}(t_1) = I_{in} \tag{12}$$

$$v_{Cr}(t_1) = V_{dc} \tag{13}$$

The solutions are determined as follows:

$$i_{Lr}(t) = I_{in} + \frac{V_0}{Z_n} \cdot \sin \omega_n (t - t_1) \tag{14}$$

$$v_{Cr}(t) = V_0 \cdot \cos \omega_n (t - t_1) \tag{15}$$

where the characteristic impedance of the active snubber network Z_n is given by

$$Z_n = \sqrt{L_r / C_r} \tag{16}$$

and the resonant angular frequency of the active snubber network ω_n is

$$\omega_n = 1/\sqrt{L_r \cdot C_r} \tag{17}$$

The time duration in this stage can be determined from the condition

$$\Delta t_{12} = t_2 - t_1 = \frac{\pi}{2} \cdot \sqrt{L_r \cdot C_r} \tag{18}$$

4) Stage 4 ($t_2 – t_3$): At $t = t_2$, the voltage $v_{Cr}(t)$ across the resonant capacitor becomes slightly negative. Therefore, the antiparallel or the body diode of the main switch *S* starts conducting. In order to achieve zero-voltage-switching (ZVS),

the main switch S should be turned on during this interval. The resonant inductor current is

$$i_{Lr}(t) = I_{Df}(t) + I_{in} \tag{19}$$

Using the initial condition $i_{Lr}(t_2) = I_{in} + V_o / Z_n$, $i_{Df}(t)$ can be solved to give

$$i_{Df}(t) = V_o / Z_n \tag{20}$$

It can be seen that the operating time in this stage is nearly zero. Thus, the time interval can be defined as

$$\Delta t_{23} = t_3 - t_2 \cong 0 \tag{21}$$

5) Stage 5 ($t_3 - t_4$): At $t = t_3$, the main switch S is turned on and the auxiliary switch S_a is turned off simultaneously. At this time, S is turned on with ZVS and the main switch current is increases linearly to I_{in}. Consequently, the energy stored in the resonant inductor L_r is transferred to the load via diode D_1. The voltage $v_{Sa}(t)$ across S_a is clamped at V_{dc} due to the conduction of D_1. The resonant inductor current $i_{Lr}(t)$ starts decreasing linearly and becomes to zero at $t = t_4$. The circuit equations and initial conditions in this stage are given as follows:

$$L_r \frac{di_{Lr}(t)}{dt} = -V_{dc} \tag{22}$$

$$C_r \frac{dv_{Cr}(t)}{dt} = 0 \tag{23}$$

$$i_{Lr}(t_3) \cong I_{in} + V_o / Z_n \tag{24}$$

$$v_{Cr}(t_3) = 0 \tag{25}$$

The solutions are determined as follows:

$$i_{Lr}(t) = -\frac{V_{dc}}{L_r} t + I_{in} + \frac{V_{dc}}{Z_n} \tag{26}$$

$$v_{Cr}(t) = 0 \tag{27}$$

The time interval of this stage can be found as

$$\Delta t_{34} = t_4 - t_3 = \frac{L_r (I_{in} + V_{dc} / Z_n)}{V_{dc}} \tag{28}$$

6) Stage 6 ($t_4 - t_5$): At $t = t_4$, the diode D_1 is turned off with ZVS naturally. During this stage, the main switch S conducts the input current I_{in}. The circuit operations are identical to the turn-on state of a conventional PWM boost converter. The switch on duration of S is given by

$$t_{on} = D \cdot T_s \tag{29}$$

where D is the main switch duty ratio and T_s is the switching time period. The time interval of this stage can be found as

$$\Delta t_{45} = t_{on} - t_{34} \tag{30}$$

7) Stage 7 ($t_5 - t_6$): At $t = t_5$, the main switch S is turned off. In this stage, C_r is linearly charged by input current I_{in} until its voltage reaches V_{dc}, the main diode D is naturally turned on. The resonant capacitor current is

$$i_{Cr}(t) = C_r \frac{dv_{cr}(t)}{dt} = I_{in} \tag{31}$$

The solution is determined as follows:

$$v_{Cr}(t) = \frac{I_{in}}{C_r} \cdot t \tag{32}$$

By using the initial condition $v_{Cr}(t_6) = V_{dc}$, the duration in this stage can be solved to give

$$\Delta t_{56} = t_6 - t_5 = \frac{C_r \cdot V_{dc}}{I_{in}} \tag{33}$$

C. Characteristic of the soft-switching converters

Due to the constant switching frequency operation, the dc characteristics of the dc-dc boost converter with active resonant snubber can be derived. Since in steady-state operation the waveform must repeat from one time period to the next, the average voltage across the inductor in steady-state operation is zero. Therefore,

$$V_{in} T_s = \int_0^{T_s} V_{Cr} dt \tag{34}$$

$$V_{in} T_s = V_{dc} \left[(1 - D - D_a) T_s + T_{01} - \frac{1}{2} T_{56} \right] + \int_{T_1}^{T_2} v_{Cr} dt \tag{35}$$

where D_a is the duty ratio of S_a. The dc voltage-conversion ratio can be defined as

$$M = \frac{V_{dc}}{V_{in}} = \frac{1}{(1 - D - D_a) + \left(T_{01} + \frac{2}{\pi} T_{12} - \frac{1}{2} T_{56} \right) / T_s} \tag{36}$$

Substituting T_{01}, T_{12} and T_{56} into Eq. (36), Therefore,

$$M = \frac{1}{(1 - D - D_a) + \left(\frac{I_{in} L_r}{V_{dc}} + \sqrt{L_r C_r} - \frac{V_{dc} C_r}{2 I_{in}} \right) / T_s} \tag{37}$$

III. Design Consideration for Soft Commutation

In this section, for ensuring adequate soft commutation, a delay time has to be determined. Then, the values of the components used in this auxiliary resonant circuit are formulated. All design constrains should be met at this point to confirm soft commutation condition.

A. Soft commutation condition

In order to achieve commutation under ZVS at turn on for the main switch S, there should have a time lag between the turn-on signals of the auxiliary switch S_a and the main switch S. Thus, the conduction time of the auxiliary switch S_a must satisfy

$$T_D \geq t_{01} + t_{12} = \frac{L_r \cdot I_{in}}{V_{dc}} + \frac{\pi}{2} \cdot \sqrt{L_r \cdot C_r} \tag{38}$$

To achieve similar conversion ratio as its hard-switching PWM counterpart, the conduction time T_D in practical design

can be specified as 5% - 10% of the switching period T_s. The proposed soft-switching can be successfully achieved by delaying the turn-on instant of main switch according to the condition of (38), the auxiliary switch conducts only during the short interval. The gating signal generating scheme to achieve this objective is depicted in figure 5.

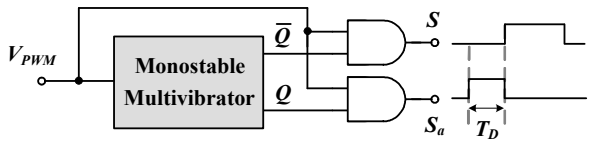

Figure 5. Control block diagram and timing of gate signals.

B. Components selections

1) Maximum resonant inductor current

In stage 3 (t_1 - t_2), the resonant inductor current $i_{Lr}(t)$ continues to increase and reaches its maximum value at $t = t_2$, one can see that the maximum value of resonant inductor current $i_{Lr,max}$ should be greater than the maximum value of the input current $I_{in,max}$. For the convenience design and energy optimization of the auxiliary resonant circuit, the maximum value of resonant inductor current can be specified as:

$$i_{Lr,\max} = a \cdot I_{in,\max} \tag{39}$$

where $1.3 < a < 1.5$ in practical design. If a is chosen to higher than 1.5, the conduction loss will be increased [5].

2) Determination of L_r and C_r

The resonant capacitor and inductor have to be designed to provide adequately soft switching for the auxiliary switch and the main switch devices. The value of L_r can be obtained by determining how fast the boost diode D_1 can be turned off. The smaller the value of L_r is specified, the larger the peak current will flow in the resonant branch. The value of the resonant capacitor C_r is the sum of the parasitic output capacitance of the main boost switch and the value of an external capacitor placed across the main switch, which is designed to control *dv/dt* of the turn-off voltage across the main switch. Hence,

$$L_r = \frac{V_{dc} \cdot t_D}{\left[(a-1)\frac{\pi}{2}+1\right] \cdot I_{in,\max}} \tag{40}$$

$$C_r = \frac{(a-1) \cdot I_{in,\max} \cdot t_D}{\left[\frac{\pi}{2}+\frac{1}{(a-1)}\right] \cdot V_{dc}} \tag{41}$$

IV. Simulation Results

To verify the operation and the performance of the proposed high-efficiency dc-dc boost converter for small grid-connected PV systems, a 40kHz, 250W PWM boost converter with active resonant snubber has been designed and simulated by Orcad PSpice®. The power circuit operates from 150Vdc voltage source and supplies 400Vdc resistive load as shown in figure 6. In the practical circuit, a diode in series with a resistor is added to absorb the high-frequency oscillation caused by the resonant inductor and parasitic capacitor of the auxiliary switch S_a. The value of the active snubber components are calculated as follows: L_r=288.3uH, C_r=0.9nF. The value of the main circuit components are L=4.97mH and C_o=100uF.

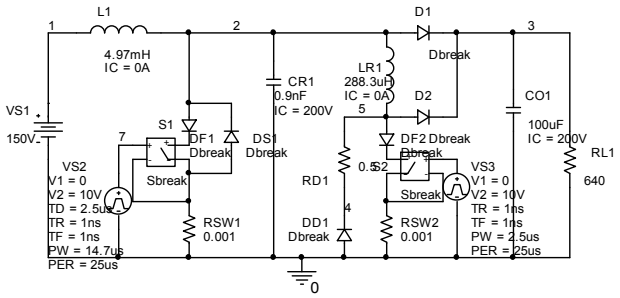

Figure 6. Orcad PSpice® simulation schematic of the proposed converter.

Fig. 7(a)-(b) shows the waveform of voltage and current of the main switch and power diode under hard-switching operation. Fig. 7(c)-(h) shows the simulation waveforms of the proposed dc-dc boost converter with active snubber during the switching period. From figure 7(d), it can be seen that the main switch S is turned on perfectly with ZVS and turned off under near ZCS. In figure 7(e), S_a is turned on under near ZCS and turned off under near ZVS. Fig. 7(f)-(g) also show the diodes D and D_1 operate with soft switching. Moreover, additional voltage and current stresses on the main switch and diode do not take place. Fig. 8 shows the efficiency comparison results. The overall efficiency of the proposed converter increases to about 94% from the value of 93% in its counterpart hard switching converter.

V. Conclusion

In this paper, an improved dc-dc boost converter with active resonant technique for small grid-connected PV systems has been proposed. An implementation of active snubber in dc-dc boost converter has been analytically analyzed and designed in detail. The operation principles and the theoretical analysis of the proposed converter in steady-state condition have been completely verified by the simulation results. The simulation results show that the active snubber can effectively suppress the switching losses of the main switch and main diode without increasing the current and voltage stresses. The snubber inductor and capacitor for the proposed converter can be precisely determined by the presented design. The overall efficiency, which is about 93% in the hard switching case, increases to about 94%.

References

[1] J. A. Gow and C. D. Manning, "Photovoltaic converter system suitable for use in small scale stand-alone or grid connected applications", IEE Proc.-Electr. Power Appl., vol. 147, pp. 535-543, Nov. 2000.

[2] K. M. Smith, Jr., and K.M. Smedley, "Engineering Design of Lossless Passive Soft Switching Methods for PWM Converters-Part I: With Minimum Voltage Stress Circuit Cells", IEEE Trans. Power Electron. vol. 16, pp. 336-344, May. 2001.

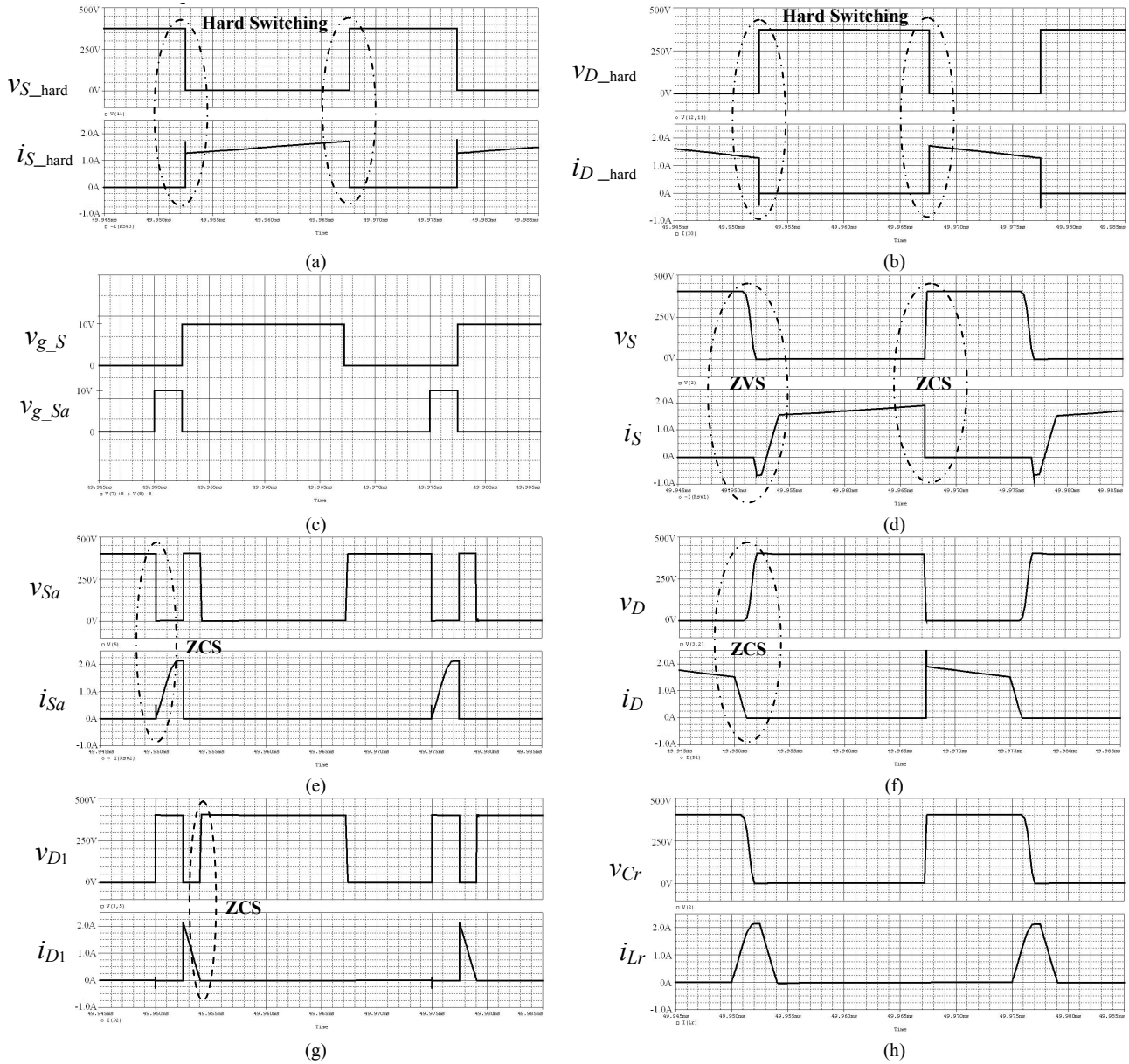

Figure 7. Simulation results of the proposed converter (a) Voltage and current of S under hard-switching condition (b) Voltage and current of D under hard-switching condition (c) Turn on signal of S and S_a (d) Voltage and current of S (e) Voltage and current of S_a (f) Voltage and current of D (g) Voltage and current of D_1 (h) Voltage of C_r and current of L_r.

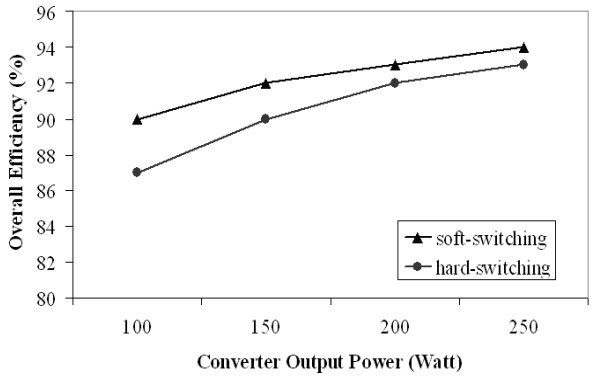

Figure 8. Converter efficiency of the proposed dc-dc boost converter.

[3] G. Hua, C. S. Leu, Y. Jiang, and F.C. Lee, "Novel zero-voltage-transition PWM converters," IEEE Trans. Power Electron., vol. 9, pp. 213–219, Mar. 1994.

[4] G. Hua, E. X. Yang, Y. Jiang, and F.C. Lee, "Novel zero-current-transition PWM converters," IEEE Trans. Power Electron., vol. 9, pp. 601–606, Nov. 1994.

[5] T.H. Chen, and C.M. Liaw, "Soft-switching inverter for electrodynamic shaker," IEE Proc.-Electr. Power Appl., vol. 146, pp. 515–523, Sep. 1999.